M&C 2017 - International Conference on Mathematics & Computational Methods Applied to Nuclear Science & Engineering, Jeju, Korea, April 16-20, 2017, on USB (2017)

Imaging of Shielded Uranium Assemblies Under Active Neutron Interrogation Using Inverse Methods

Aaron B. Nowack*, Seth M. McConchie†, Jason P. Hayward*,†

*Department of Nuclear Engineering, The University of Tennessee, Knoxville, Knoxville, TN
†Nuclear Materials and Characterization Group, Oak Ridge National Laboratory, P.O. Box 2008, Oak Ridge, TN
anowack@vols.utk.edu, mcconchiesm@ornl.gov, jhayward@ornl.gov

Abstract - *The point kinetics model for the emission of neutrons relies on several assumptions including that all neutrons are emitted from a single location. With the advancement of active neutron imaging systems, methods for determining the amount of fissile material, enrichment, and multiplication are constrained by the exclusion of extended geometry in the point kinetics model. This work begins to bridge between point kinetics and image reconstruction methods so that estimates of enrichment and multiplication can be derived throughout a geometry of large and shielded fissile materials. A theory for building this image reconstruction method is developed and inverse problem methods are applied to reconstruct the total and fission neutron macroscopic neutron cross sections for simulated data.*

I. INTRODUCTION

The current state of the art in characterization of uranium assemblies relies on either point kinetics, a simplified version of nuclear transport theory, or imaging systems using either passive or active neutron interrogation. Measurements taken by Active Well Coincidence Counters (AWCC) are excellent in characterizing small arrangements of unshielded uranium in the point kinetics model. Tagged neutron interrogation imagers, such as the Associated Particle Neutron Imaging System (APNIS) developed at Oak Ridge National Laboratory, have enhanced the spatial resolution of neutron imaging measurements [1]. However, for characterizing the properties of large and fissile assemblies of uranium surrounded by shielded materials, both AWCC and current neutron imaging methods have limitations. By developing algorithms which incorporate a model of neutron transport directly into imaging reconstruction methods, the state of the art for characterizing large uranium assemblies can be advanced.

AWCC analysis methods rely on a point kinetics framework in which all fission emissions are assumed to have originated at a single position [2]. This simplification leads to a small set of equations which return uranium characteristics from neutron coincidence and multiplicity measurements. Errors are primarily due to the inability to account for the geometric dependence of the assembly which can be mitigated by limiting to small sample sizes. When the bias of a known geometry has been measured beforehand, a predetermined systematic correction can be applied [3]. Conversely, estimating uranium characteristics from imaged data acquired by tagged neutron interrogation systems relies on detailed and extensive Monte Carlo studies requiring several skilled scientists and excessive computation times [4]. Neither of these methods allow for the rapid, in-field use on unknown items needed for scenarios in nuclear material control and accountability.

To bridge between point kinetics and the need for Monte Carlo studies a framework which incorporates the response of neutrons created from induced fission chains into image reconstruction has been developed. This framework begins with the transmission of an initial neutron from active interrogation and calculates the probabilities for detecting either one or additional neutrons emerging from the shielded assembly. The probability for creating a single fission or a fission chain is then related to the detection of one or more neutrons in a neutron imaging detector array. Inverse problem methods are used to reconstruct the geometry and characteristics of fissile material providing a better estimate for uranium characteristics in large and shielded assemblies.

A toolkit for quickly modelling transport of interrogating neutrons through material has been developed. The purpose is to calculate the response of voxels of materials quickly to be used in reconstruction of an entire assembly. It is a 2D neutron transport model which calculates the probability of a neutron interacting – either being removed or initiating a fission over a path in an assembly of different materials. This is done by decomposing the geometry of the assembly into a series of discrete line segments as shown in Figure 1. Each line segment stores the direction of a normal vector and the macroscopic neutron cross sections on each opposite side of the line segment.

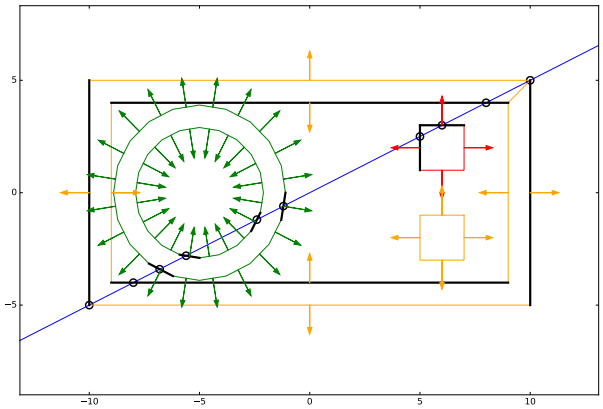

Fig. 1. A 2D geometry displaying from above the boundary of a uranium casting (green) surrounded by other non fissile materials. The arrows represent the normal vector for each line segment. An intersecting ray is shown (blue) with intersecting segments and intersections outlined.

This toolkit is used to create to create simulated data and responses for transmitted neutrons and those from induced fission. Inverse methods are then used with the responses to estimate the fissile material from the data.

1. Overview

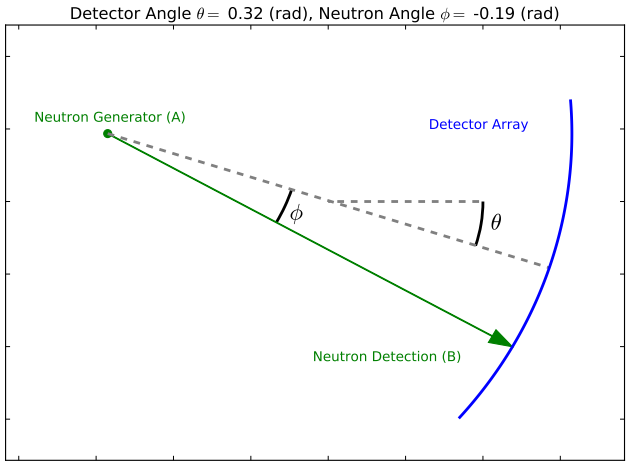

Fig. 2. A diagram showing the neutron starting position (A), travelling to the detector array (B). The interrogating neutron path is determined by the angle relative to the detector array center ϕ, and the relative angle θ of the detector array with respect to the x-axis.

The model begins with the transmission of an active interrogation neutron with fixed energy $E = 14.1$ MeV, corresponding to a DT neutron generator. The neutron direction is measured and begins travel along a ray AB where A is the neutron generator location and B a later position of the neutron if unimpeded by material. A diagram of the setup is shown in Figure 2. In practice the angle ϕ is measured using a position sensitive alpha detector behind the DT neutron generator [1].

Opposite of the neutron generator is a position sensitive neutron detector array measuring whether the neutron was transmitted or impeded. This model assumes fission neutrons have been accurately identified, distinguished from scatter neutrons by kinematics, timing, and energy.

Two additional assumptions in this work are that the only fissile material present is enriched uranium, and a simplification that all neutron fission chains are a fixed length ν_n which is only valid for low enriched materials. Future extensions of this model will relax this assumption.

The observed quantities are, for an interrogating neutron travelling in a known direction, the probability across the detector plane of recording a transmitted neutron and of detecting one, two, or more fission neutrons. The model relates these with the unknown neutron attenuation coefficient μ and the portion due to induced fission reactions μ_f. Both μ and μ_f are at the interrogating neutron energy and both are recovered as a two dimensional image of the material.

Assuming the fissile material is enriched uranium only, μ_f can be related to the percentage of enrichment, f_{235}, through the following expression

$$f_{235} = \frac{2A_U\mu_f}{\sigma_{235}N_a\rho} - 1 \tag{1}$$

where A_U is the isotopic weight of uranium, σ_{235} the microscopic uranium cross section, N_a avogadro's number, and ρ the bulk density.

II. THEORY

1. Neutron Detection Model

A. Transmitted Neutron Detection

For material with a total macroscopic cross section for neutrons, μ, the probability of transmission for a path (A, B),

$$\mathrm{P}_{\text{transmission}}(A, B) = e^{-\int_A^B \mu(x,y)ds} \tag{2}$$

can be computed quickly by calculating the intersections along path A,B with material boundaries decomposed as line segments as shown in Figure 1. With the points of intersections known, the computation for the attenuation integral can be calculated directly as a sum [5],

$$e^{-\int_A^B \mu(x,y)ds} = \sum_i |I_i - B| \, (\mu_{i,in} - \mu_{i,out}) \, \mathrm{sgn}(A - I_i \cdot N_i) \tag{3}$$

where I_i is the ith intersection position, $\mu_{i,in}$ and $\mu_{i,out}$ the attenuations on either side of the material boundary, and N_i the normal vector at the intersection from the material surface boundary.

Measuring $P_{\text{transmission}}$ over the detector array for varying orientations gives a sinogram over ϕ and θ as shown in Figure 3 for the object in Figure 1.

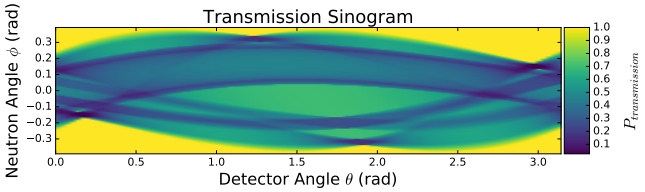

Fig. 3. A transmission sinogram of the object in Figure 1. The sinogram is done over the (θ, ϕ) space as defined in Figure 2.

B. Induced Fission Neutron Detection

In tagged neutron interrogation systems a neutron generated from a source, located at $S(\theta)$, travels in a measured direction ϕ. Opposite the source $S(\theta)$ lies an array of neutron imaging detectors, $D(\theta, \phi)$. As the neutron travels into the assembly it can either be removed by absorption or scattering, or for fissile materials it may create a fission or fission chain at a location (x, y). This creates additional neutrons which can be measured by $D(\theta, \phi)$. The probability for detecting k neutrons generated by a fission at (x, y) can be expressed as:

$$\mathrm{P}(x, y \,|\, k) = \mathrm{P}_{\text{in}}(x, y \,|\, S(\theta)) \, \mathrm{P}_{\text{fission}}(x, y) \, \mathrm{P}_{\text{out}}(x, y \,|\, k) \tag{4a}$$

$$\mathrm{P_{in}}(x,y\,|\,S(\theta)) = e^{-\int_{S(\theta)}^{(x,y)}\mu(s)\,ds} \tag{4b}$$

$$\mathrm{P_{fission}}(x,y) = \mu_f(x,y)\,ds \tag{4c}$$

where $\mathrm{P_{in}}$ is the probability of neutron transmission into the assembly from the neutron source $S(\theta)$ to (x,y), and $\mathrm{P_{fission}}$ is for the source neutron initiating a fission at (x,y) within a material with a macroscopic fission cross section μ_f.

The transport of k fission neutrons out of the assembly to an arrangement of detectors $D(\theta,\phi)$ is expressed as

$$\mathrm{P_{out}}(x,y\,|\,k) = \sum_n \nu_n(x,y)\binom{n}{k}\mathrm{P_{detect}}(x,y)^k(1-\mathrm{P_{detect}}(x,y))^{n-k}. \tag{5}$$

The number distribution of neutrons from a fission or fission chain within fissile material initiated by a source neutron at (x,y) is $\nu_n(x,y)$. For a single fission this is just the Terrell distribution for that isotope [6]. For fission chains, the effects of self multiplication and neutron reflection by surrounding materials results in a wider distribution compared with the Terrell distribution.

The probability of neutron escape (5) is weighted by a binomial distribution of each fission neutron escaping the material and being detected with independent probability $\mathrm{P_{detect}}$. The detection probability includes the transport out of the material weighted by the detector solid angle fraction Θ integrated over the detector plane:

$$\mathrm{P_{detect}} = \int \Theta(x,y,D(\theta,\phi))\,e^{-\int_{(x,y)}^{D(\theta,\phi)}\mu(s)\,ds}d\phi \tag{6}$$

For $\mathrm{P_{detect}}$ and $\mathrm{P_{in}}$, the path attenuation integrals are calculated using the 2D neutron transport toolkit used in Figure 3.

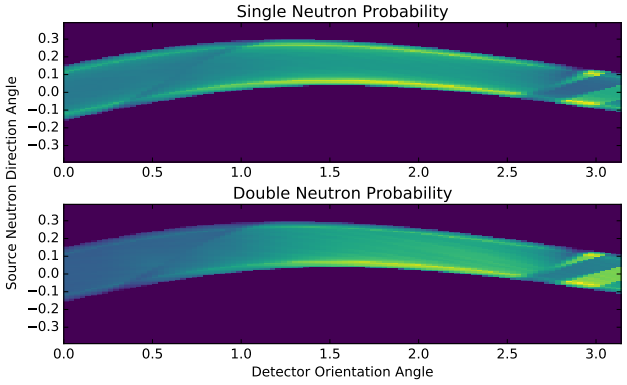

Fig. 4. The total probability of detecting either one (top) or two (bottom) neutrons from fission for a given orientation of source neutron direction. The measurement is based on the geometry shown in Figure 1. The colorscale is a relative probability intensity of $P(x,y\,|\,k)$ for $k = 1,2$

A measurement of the neutron probability for $k = 1,2$ (4a) is shown in Figure 4. This is for the uranium casting in Figure 1 irradiated with a fan beam of source neutrons and measured over a scan of 180 degrees.

III. RESULTS AND ANALYSIS

1. Model Response

For an unknown assembly of shielded uranium it is desired to reconstruct an unknown image, X, of both the total macroscopic cross section $\mu(x,y)$ and the component due to fission $\mu_f(x,y)$. This is done by decomposing the image into an array of pixels, applying the neutron detection model on each pixel, and determining which arrangement best matches the data by using inverse problem methods.

Three response matrices are calculated for the transmission, single, and double neutron measurements. The measurement can be represented by the linear system:

$$A_{\mathrm{response}}\,X_{\mathrm{assembly}} = Y_{\mathrm{measurement}} \tag{7}$$

due to the linear properties of the radon integral transform for the transmission measurement [7], and the linear coefficient of μ_f in Equation 4c of the neutron single and double measurements. To recover an unknown configuration X_{assembly} many inverse methods such as the Moore-Penrose pseudo-inverse or Tikhonov Regularization can be applied.

A. Transmission Model Response

The modelling of the transmission response $A^{\mathrm{trans}}_{(\theta,\phi)}$ is done by discretizing the image plane into a grid of pixels, where each pixel is a defined unit size with attenuation of 1 unit path length as shown in Figure 5. For each pixel the attenuation is calculated for different orientations of the source neutron position and detector array angles (θ,ϕ). The radon transform of each pixel is stored over all neutron source and detector orientations. Any measured radon transform can then be decomposed into weighted sums of the radon model response pixels.

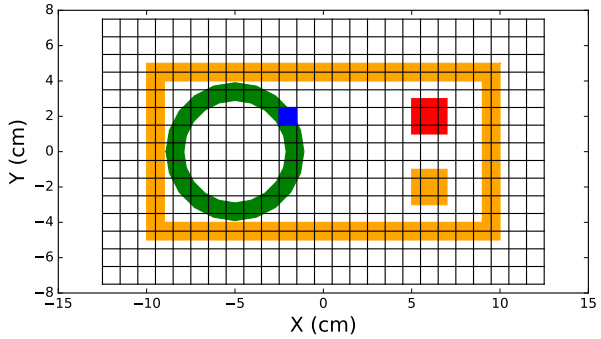

Fig. 5. The decomposition of the image space into pixels, a single pixel is shown in blue. Transmission responses are created for each individual pixel. For illustration the pixels are enlarged by a factor of four.

B. Fission Model Response

The fission neutron single ($k = 1$) and double ($k = 2$) responses $A^{k=1}_{(\theta,\phi)}, A^{k=2}_{(\theta,\phi)}$ use the same setup as the transmission response in Figure 5. Since the $\mathrm{P_{in}}$ and $\mathrm{P_{out}}$ terms in the single and double fission neutron probabilities rely on calculating

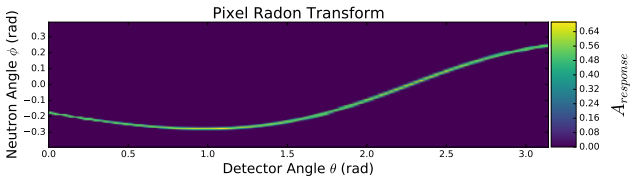

Fig. 6. The transmission response matrix $A^{\text{trans}}_{(\theta,\phi)}$ for the pixel shown in Figure 6.

the attenuation to and from a point (x, y) the transmission reconstruction must be done first. The response for each pixel is calculated for each orientation $R(\theta, \phi)$ of the neutron source and detector array as

$$A^{k}_{(\theta,\phi)} = \int_{R(\theta,\phi)} \mathrm{P}(x, y \,|\, k) = \int_{R(\theta,\phi)} \mathrm{P}_{\text{in}}(x, y \,|\, S(\theta))\, \mathrm{P}_{\text{out}}(x, y \,|\, k)\, \mu_f(x, y)\, ds \quad (8)$$

where the representation of $\mathrm{P}_{\text{fission}}$ has been substituted. The path integral is over the portion of the neutron source path which intersects the response pixel. The orientation of the neutron path $R(\theta, \phi)$ is determined by the angles as shown in Figure 2. The elements of $A^{k}_{(\theta,\phi)}$ are normalized such that a value of 1 indicates all neutron attenuation in the pixel is due to fission, $\mu_f(x, y) = \mu(x, y)$. The response of detecting a single fission neutron ($k = 1$) or a pair of fission neutrons ($k = 2$) is calculated over all neutron source and detector orientations for every pixel.

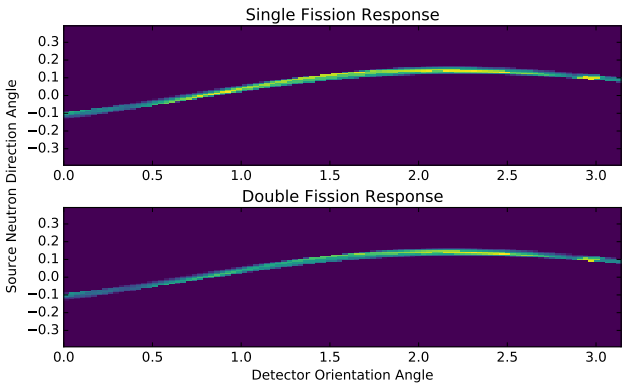

Fig. 7. $A^{k=1}_{(\theta,\phi)}$ (above) and $A^{k=2}_{(\theta,\phi)}$ (below) are shown for a pixel. The overall shape is from the transmission portion, the highlighted region toward the center from the increased detector solid angle for those orientations, and the banding due to self shielding of the assembly by surrounding materials.

With a set of response matrices for the transmission, single fission, and double fission neutrons calculated, methods from solving inverse problems are used to recover the unknown image of the material and the fissile component.

2. Transmission Estimate

The transmission measurement is used with the previously described $A^{\text{trans}}_{(\theta,\phi)}$ for transmission to recover the image of the total cross-section μ. However, since $A^{\text{trans}}_{(\theta,\phi)}$ is sparse and ill-conditioned a unique solution to Equation 7 will not exist [8]. To favor solutions which are stable, Tikhonov Regularization is applied where a penalty, α, on the norm of the unknown image is applied. The reconstruction of μ reduces to a least squares problem

$$\min \left\| \begin{bmatrix} A^{\text{trans}}_{(\theta,\phi)} \\ \alpha\, I \end{bmatrix} \mu(x, y) - \begin{bmatrix} Y_{\text{trans}} \\ 0 \end{bmatrix} \right\|^2_2 \quad (9)$$

where $A^{\text{trans}}_{(\theta,\phi)}$ is from Figure 6, Y_{trans} is the data as shown in Figure 3.

The solution can be calculated analytically as

$$\hat{\mu}(x, y) = \left(A^{\text{trans}\,T}_{(\theta,\phi)} A^{\text{trans}}_{(\theta,\phi)} + \alpha^2 I \right)^{-1} A^{\text{trans}\,T}_{(\theta,\phi)} Y_{\text{trans}} \quad (10)$$

where α is a penalty coefficient [9].

The result of applying Tikhonov Regularization for the transmitted neutrons is shown in Figure 8. Once a response matrix has been calculated a reconstruction can be done easily for many images. More advanced methods such as Total Variation Imaging can also be applied for images of several homogenous materials [8].

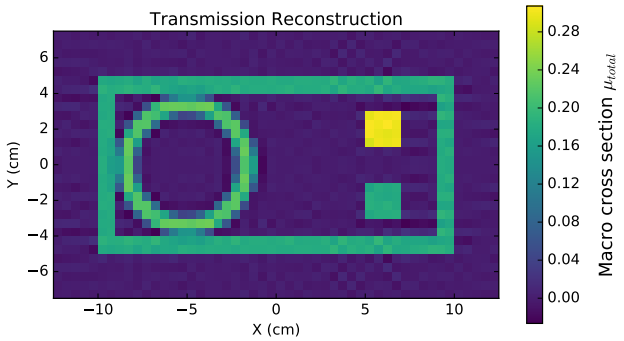

Fig. 8. Reconstruction of the total macroscopic neutron attenuation cross section using the Tikhonov reconstruction of Equation 10.

3. Single and Double Neutron Estimate

The same Tikhonov reconstruction as used for transmission is then applied on the single and double detected fission neutron measurements and responses. This is done jointly by solving for a single image of the μ_f/μ_{total} fraction with the single and double fission neutron responses shown in Figure 7. The least squares system to solve is

$$\min \left\| \begin{bmatrix} A^{\text{k=1}}_{(\theta,\phi)} \\ A^{\text{k=2}}_{(\theta,\phi)} \\ \alpha\, I \end{bmatrix} \frac{\mu_f}{\mu}(x, y) - \begin{bmatrix} Y_{\text{k=1}} \\ Y_{\text{k=2}} \\ 0 \end{bmatrix} \right\|^2_2 \quad (11)$$

with an analytic solution,

$$(\hat{\mu}_f/\mu)(x, y) = \left(A^{\text{k=1}\,T}_{(\theta,\phi)} A^{\text{k=1}}_{(\theta,\phi)} + A^{\text{k=2}\,T}_{(\theta,\phi)} A^{\text{k=2}}_{(\theta,\phi)} + \alpha^2 I \right)^{-1} \left(A^{\text{k=1}\,T}_{(\theta,\phi)} Y_{\text{k=1}} + A^{\text{k=2}\,T}_{(\theta,\phi)} Y_{\text{k=2}} \right) \quad (12)$$

The resulting image of the μ_f/μ fraction is shown in Figure 9. The fission component of the macroscopic cross section is reconstructed for the uranium casting and in the correct location and at the correct simulated enrichment of 10%. These images use the Terrel fission distribution for ν_n [6].

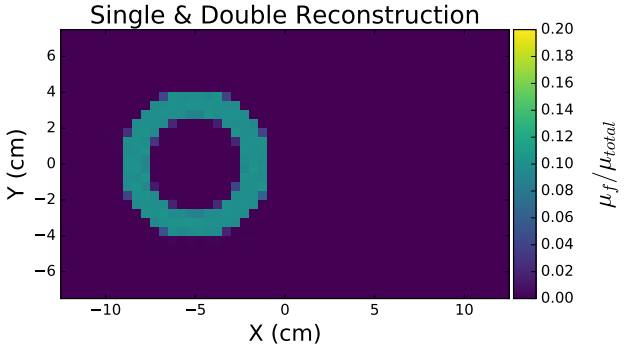

Fig. 9. Reconstruction of μ_f/μ_{total} fraction using the solution in Equation 12. The reconstruction correctly shows the simulated enriched uranium casting cross-section at an enrichement level of 10%.

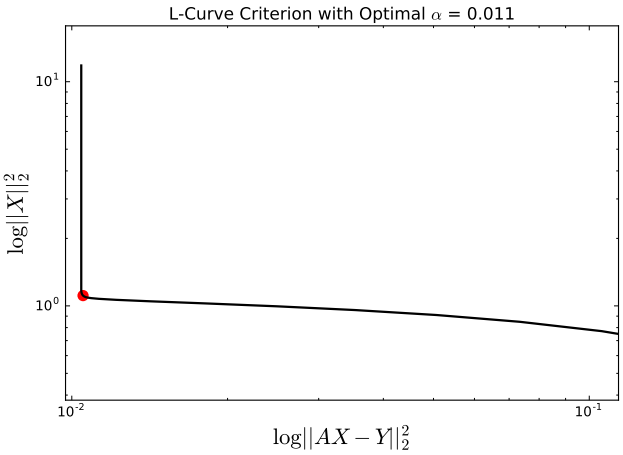

Fig. 10. L-Curve criterion plot for the reconstruction of Figure 9. The red dot corresponds to the point of highest curvature and is the best choice for α.

For both reconstructions in Figures 8 and 9 the α parameter is an unknown variable. In practice it is common to determine an optimal α value through the L-Curve criterion [8], in which the log of both the solution norm, and the norm residual are plotted against each other as a function of α. The optimal α is at the point of highest curvature as shown in Figure 10.

IV. CONCLUSIONS

This work has developed an image reconstruction method which incorporates neutron transport. This extends beyond the simpler transmission model and reconstructs single and double neutron measurements from induced fission.

Extensions of this work will allow ν_n to vary continuously according to a free parameter relating to fission chain length, which will account for additional fission neutrons created from self multiplication and reflection by surrounding materials. Non-linear methods must be applied for self multiplication and reflection as μ_f will no longer be a linear coefficient in Equation 4c.

V. ACKNOWLEDGMENTS

This material is based upon work supported by a U.S. Department of Energy, National Nuclear Security Administration grant DE-NA0002493.

REFERENCES

1. P. A. HAUSLADEN, M. A. BLACKSTON, J. A. MULLENS, S. MC CONCHIE, J. T. MIHALCZO, P. R. BINGHAM, M. NANCE ERICSON, and L. FABRIS, "Induced-Fission Imaging of Nuclear Material," (2010).
2. K. BÖHNEL, "The Effect of Multiplication on the Quantitative Determination of Spontaneously Fissioning Isotopes by Neutron Correlation Analysis," *NSE*, **90**, *1*, 75–82 (May 1985).
3. N. ENSSLIN, W. GEIST, M. KRICK, and M. PICKRELL, "Active Neutron Multiplicity Counting," Tech. Rep. LA-UR-07-1403, Los Alamos Scientific Laboratory.
4. J. T. MIHALCZO, P. R. BINGHAM, M. A. BLACKSTON, J. M. CRYE, B. R. GROGAN, P. HAUSLADEN, S. M. MCCONCHIE, and J. A. MULLENS, "Fast-Neutron Imaging with API DT Neutron Generators," (Jan 2012).
5. N. FREUD, P. DUVAUCHELLE, J. LÃL'TANG, and D. BABOT, "Fast and robust ray casting algorithms for virtual X-ray imaging," *Nuclear Instruments and Methods in Physics Research Section B: Beam Interactions with Materials and Atoms*, **248**, *1*, 175 – 180 (2006).
6. J. TERRELL, "Distributions of Fission Neutron Numbers," *Phys. Rev.*, **108**, *3*, 783–789 (Nov 1957).
7. T. S. DURRANI and D. BISSET, "The Radon transform and its properties," *Geophysics*, **49**, *8*, 1180–1187 (1984).
8. R. C. ASTER, C. H. THURBER, and B. BORCHERS, "Parameter estimation and inverse problems," (2013).
9. G. H. GOLUB and C. F. V. LOAN, "Matrix Computations," (1989).